On satisfying the radiation condition in free-surface flows

B. J. BINDER, J.-M. VANDEN-BROECK and F. DIAS

Journal of Fluid Mechanics / Volume 624 / April 2009, pp 179 - 189
DOI: 10.1017/S0022112008005028, Published online: 30 March 2009

J. Fluid Mech. (2009), *vol.* 624, *pp.* 179–189.
doi:10.1017/S0022112008005028 Printed in the United Kingdom

On satisfying the radiation condition in free-surface flows

B. J. BINDER[1], J.-M. VANDEN-BROECK[2]† AND F. DIAS[3]

[1]School of Mathematical Sciences, University of Adelaide, Adelaide, South Australia, 5005, Australia

[2]Department of Mathematics, University College London, London WC1E 6BT, UK

[3]CMLA, ENS Cachan, CNRS, PRES UniverSud, 61 Av. President Wilson, F-94230 Cachan, France

(Received 2 June 2008 and in revised form 17 November 2008)

Binder & Vanden-Broeck (2005) showed there are no subcritical or critical solutions satisfying the radiation condition for steady flows past a flat plate. By using a weakly nonlinear analysis, it is shown that such flows exist for a curved plate. Fully nonlinear solutions are computed by a boundary integral equation method, and new nonlinear solutions for supercritical and generalized critical flows past a curved plate are presented.

1. Introduction

The problem of free-surface flows past different types of disturbances in an open channel is classical. The disturbances can be (i) a submerged obstacle on the bottom of the channel (Forbes 1998; Dias & Vanden-Broeck 2002; Binder, Dias & Vanden-Broeck 2005), (ii) a step in the bottom of the channel (King & Bloor 1987; Binder, Dias & Vanden-Broeck 2006) and (iii) an obstruction in the free surface, which is usually a plate. This models flows past surfboards (Vanden-Broeck & Keller 1989; Binder & Vanden-Broeck 2005), planing hydrofoils (Fridman & Tuck 2006), and sluice gates (see Budden & Norbury 1977; Vanden-Broeck 1997; Binder & Vanden-Broeck 2005 and the references cited in these papers). In this paper we discuss new solutions when the obstruction in the free surface is a curved plate.

In all the solutions presented in this paper, the flow is assumed to have constant velocity U and constant depth H far downstream. We define the Froude number

$$F = \frac{U}{(gH)^{1/2}}. \tag{1.1}$$

Here g is the acceleration due to gravity. Far upstream the flow can contain a train of waves or be a uniform stream with constant velocity V and constant depth D. In the latter case we introduce an additional Froude number

$$F^* = \frac{V}{(gD)^{1/2}}. \tag{1.2}$$

In the case of a single submerged obstacle or a step in the bottom of the channel four basic flow types have been identified. The first type is a supercritical flow with

† Email address for correspondence: broeck@math.ucl.ac.uk

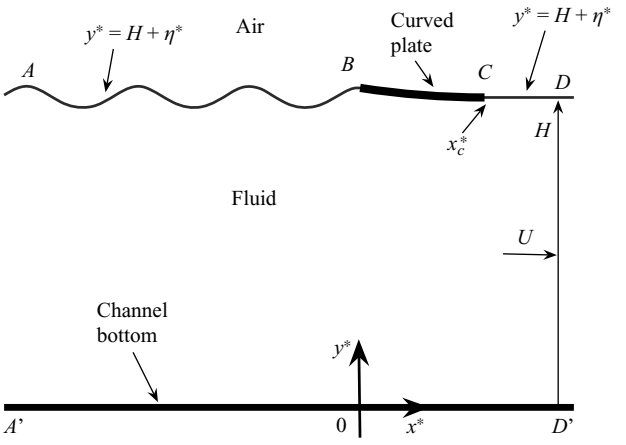

FIGURE 1. Sketch of the flow past a curved plate.

$F = F^* > 1$. The second is a subcritical flow with $F < 1$ and a train of waves far upstream. (Physical solutions satisfying the radiation condition are then obtained by reversing the direction of the flow.) The third is a critical flow with $F > 1$ and $F^* < 1$. The fourth is a generalized critical flow characterized by $F > 1$ and a train of waves far upstream. The first three basic flows are classical. The fourth type was first calculated by Dias & Vanden-Broeck (2002). The generalized critical flows (i.e. the solutions of the fourth type) lack physical meaning because the waves do not satisfy the radiation condition which requires that there be no energy coming from infinity. However Dias & Vanden-Broeck (2004) showed that the radiation condition can be satisfied by introducing a second obstacle in the channel. The waves can then be trapped between the two obtacles.

Vanden-Broeck (1997) and Binder & Vanden-Broeck (2005) showed that for a single flat plate (e.g. a surfboard and a sluice gate) there are solutions of the fourth type but no solutions of the third type. Furthermore Binder *et al.* (2005) found that there are no solutions of the second type: all the subcritical solutions have trains of waves far upstream and far downstream and do not therefore satisfy the radiation condition. Dias & Vanden-Broeck (2004) and Binder & Vanden-Broeck (2007) showed that the waves which do not satisfy the radiation condition in the subcritical solutions and the solution of the fourth type can be eliminated by introducing a second disturbance in the channel. The subcritical flows and the flow of the fourth type then become flows of the second and third type respectively.

In this paper we use a weakly nonlinear theory to show that solutions for subcritical and critical flows can be constructed without introducing a second disturbance into the channel, provided the flat plate is replaced by a curved plate. In addition we use a boundary integral equation method to compute new fully nonlinear solutions for supercritical and generalized critical flow past a curved plate. These numerical results are consistent with previous computations by Asavanant & Vanden-Broeck (1994).

The boundary integral equation method and the weakly nonlinear theory are described in § 2. The results are presented in § 3.

2. Formulation

Consider the steady two-dimensional irrotational flow of an inviscid and incompressible fluid past a curved plate in an open channel (see figure 1). The

fluid is bounded from below by the bottom of the channel $A'D'$ and from above by the two free surfaces AB and CD and the curved plate BC. A system of Cartesian coordinates (x^*, y^*) is defined with the x^*-axis along the bottom of the channel and the y^*-axis passing through the separation point B ($x^* = 0$) of the curved plate. The acceleration due to gravity, g, is acting in the negative y^* direction. The horizontal distance from the y^*-axis to the separation point C is denoted by x_c^*. The flow is assumed to separate tangentially from the curved plate BC. As $x \to \infty$ the flow approaches a uniform stream with constant velocity U and constant depth H. The equation of the streamline $ABCD$ is $y^* = H + \eta^*$, where η^* is the elevation of the free surface on top of the level H.

Dimensionless quantities $(x, y, \eta, x_c) = (x^*, y^*, \eta^*, x_c^*)/H$ and $(u, v) = (u^*, v^*)/U$ are defined by taking H as the reference length and U as the reference velocity. Here, u^* and v^* are the horizontal and vertical components of the velocity. The boundary integral equation method used to solve the fully nonlinear problem and the weakly nonlinear theory are described in §§ 2.1 and 2.2 respectively.

2.1. *Nonlinear boundary integral equation*

The numerical procedure follows closely that used in Vanden-Broeck (1997) and Binder & Vanden-Broeck (2005). The reader is referred to these papers for further details.

We introduce the complex potential function f and the complex velocity w:

$$f = \phi + \mathrm{i}\psi, \quad w = \frac{\mathrm{d}f}{\mathrm{d}z} = u - \mathrm{i}v. \tag{2.1}$$

Without loss of generality we choose $\psi = 0$ on the free-surface streamline $ABCD$, and it follows that $\psi = -1$ on the channel bottom streamline $A'D'$. We choose $\phi = 0$ ($x = 0$) at B and let $\phi = \phi_c$ ($x = x_c$) at C. We define the function $\tau - \mathrm{i}\theta$ as

$$w = u - \mathrm{i}v = e^{\tau - \mathrm{i}\theta} \tag{2.2}$$

and obtain the integral equation

$$\tau(\phi) = \int_{-\infty}^{\infty} \frac{\theta(\phi_0)\, e^{\pi\phi_0}}{e^{\pi\phi_0} - e^{\pi\phi}}\, \mathrm{d}\phi_0, \tag{2.3}$$

which relates the values of τ and θ along $\psi = 0$. The integral in (2.3) is a Cauchy principal value.

On the free surfaces, the dynamic boundary condition gives

$$e^{2\tau} + \frac{2}{F^2} y = 1 + \frac{2}{F^2} \quad \text{on} \quad AB \quad \text{and} \quad CD. \tag{2.4}$$

We prescribe the shape of the curved plate by writing

$$\frac{\mathrm{d}y}{\mathrm{d}x} = \frac{\mathrm{d}\eta}{\mathrm{d}x} = \tan\theta = G(\eta) \quad \text{on} \quad BC, \tag{2.5}$$

where $G(\eta)$ is given.

Finally we relate the values of x and y on $\psi = 0$ by integrating numerically the identity

$$x_\phi + \mathrm{i}y_\phi = \frac{1}{u - \mathrm{i}v} = e^{-\tau + \mathrm{i}\theta} \tag{2.6}$$

and equating real and imaginary parts. This gives a parametric representation $x = x(\phi)$, $y = y(\phi)$ for the streamline $\psi = 0$.

Equations (2.3)–(2.6) define a nonlinear integro-differential equation for the unknown function $\theta(\phi)$ on $ABCD$. This equation is discretized and the resulting equations are solved by Newton's method.

2.2. *Weakly nonlinear theory*

Several investigators (Shen 1995; Dias & Vanden-Broeck 2002; Binder *et al.* 2005 and others) have derived a forced Korteweg–de Vries equation to model the flow past an obstacle on the bottom of a channel. This weakly nonlinear theory is asymptotically valid for F close to one and for small disturbances.

Binder & Vanden-Broeck (2005) derived the corresponding weakly nonlinear theory for flows past a flat plate. They showed that the flow is described on the free surfaces AB and CD by the (integrated) Korteweg–de Vries equation

$$\eta_x^2 = 6(F-1)\eta^2 - 3\eta^3 + C_w \quad \text{on} \quad AB \quad \text{and} \quad CD. \tag{2.7}$$

Here C_w is a constant. Along the flat plate

$$\eta_x = s, \tag{2.8}$$

where s is the (constant) slope of the flat plate. Exact solutions can then be constructed in the phase plane η_x versus η. The idea is to combine the trajectories associated with (2.7) with horizontal jumps corresponding to (2.8).

Here we extend the approach from flat plates to curved plates by replacing (2.8) by (2.5). The main difference is that the jumps are no longer horizontal in the phase plane.

We shall consider two choices for the function $G(\eta)$:

$$G_1(\eta) = \alpha\eta + \beta, \quad G_2(\eta) = \pm(4\gamma\eta)^{1/2}. \tag{2.9}$$

Here α, β and γ are given constants.

Equation (2.5) can be integrated to give the shape of the plate. For example integrating (2.5) with the choice G_1 (2.9) yields

$$\eta = ce^{\alpha x} - \frac{\beta}{\alpha} \quad \text{on} \quad BC, \tag{2.10}$$

where $c = \eta(0) + \beta/\alpha$ is a constant of integration. The value of x at C is given by

$$x_c = \frac{1}{\alpha}\log\left[\frac{\alpha\eta(x_c)+\beta}{\alpha\eta(0)+\beta}\right] = \frac{1}{\alpha}\log\left[\frac{\eta_x(x_c)}{\eta_x(0)}\right]. \tag{2.11}$$

For geometric simplicity we shall require $x_c > 0$ in all the calculations.

Detailed weakly and fully nonlinear solutions are presented in the next section.

3. Results

We shall describe the solutions corresponding to supercritial flows, generalized critical flows, subcritical flows and critical flows in four separate sections.

3.1. *Supercritical flow*

In this section we describe supercritical flows with $F = F^* > 1$ corresponding to the curved plate G_1 (2.9). The phase plane (η, η_x) corresponding to (2.7) for a typical value $F = F^* = 1.2$ is shown in figure 2(*b*). There is saddle point at $(0, 0)$ and a centre at $(4(F-1)/3, 0)$. The inner closed trajectories are periodic waves. The outer closed trajectory is a homoclinic trajectory describing a solitary wave. It corresponds to the choice $C_w = 0$ in (2.7).

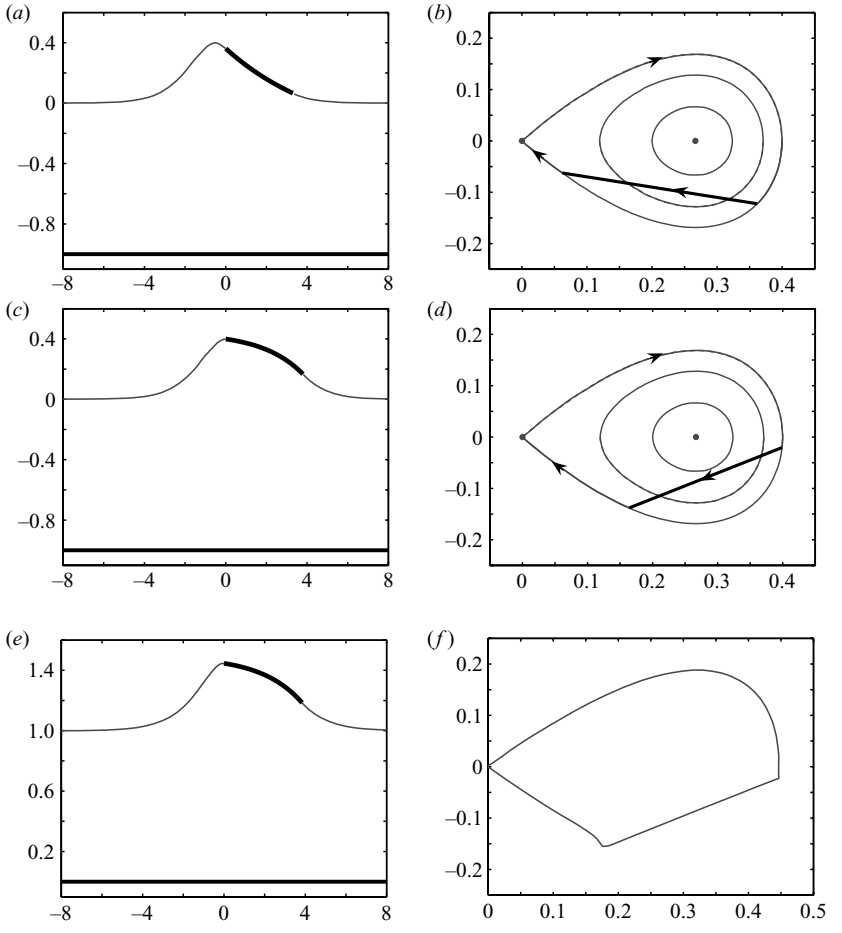

FIGURE 2. Supercritical flow, $F = 1.20$. The shape of the curved plate is defined by G_1 (2.9). (*a*) Weakly nonlinear profile: $\alpha = -0.20$, $\beta = -0.05$, $\eta(0) = 0.36$, $\eta(x_c) = 0.06$ and $x_c = 3.37$. (*b*) Weakly nonlinear phase portrait for (*a*). (*c*) Weakly nonlinear profile: $\alpha = 0.50$, $\beta = -0.22$, $\eta(0) = 0.39$, $\eta(x_c) = 0.16$ and $x_c = 3.45$. (*d*) Weakly nonlinear phase portrait for (*c*). (*e*) Nonlinear profile: $\alpha = 0.50$, $\beta = -0.25$, $y(0) = 1.45$, $y(x_c) = 1.18$ and $x_c = 3.85$ ($\phi_c = 2.80$). (*f*) Nonlinear phase trajectory for (*e*).

To construct a weakly nonlinear solution we start at the saddle point in the phase plane and move along the homoclinic orbit in a clockwise direction. At B where the upstream free surface separates from the curved plate we move along the straight line G_1 (2.9) until we rejoin the homoclinic orbit at C where the downstream free surface separates from the curved plate. We then continue along the homoclinic orbit in the clockwise direction and finish at the saddle point in the phase plane (figure 2*b*, *d*).

The number of independent parameters for a solution is three. They can be taken as $F > 1$ which provides the general layout of the phase plane diagram and α and β which determine where the straight line is in the phase plane. The values of $\eta(0)$, $\eta_x(0)$, $\eta(x_c)$, $\eta_x(x_c)$ and x_c must then come as part of the solution.

We present in figure 2(*a*, *c*) typical weakly nonlinear profiles. The corresponding phase plane portraits are shown in figure 2(*b*, *d*).

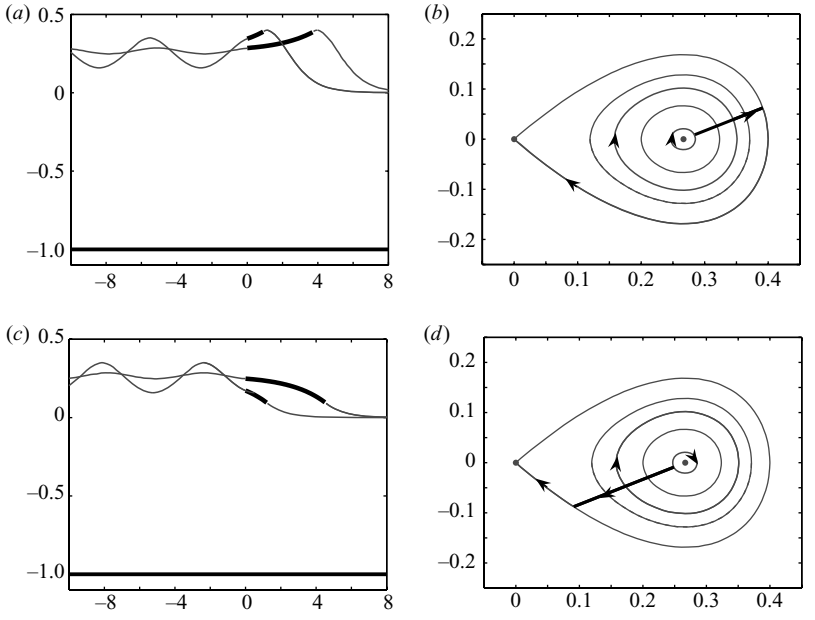

FIGURE 3. Generalized critical flow: $F = 1.20, \alpha = 0.50$ and $\beta = -4/30$. The shape of the curved plate is defined by G_1 (2.9). (*a*) Weakly nonlinear profiles; $\eta(x_c) = 0.39$. The profile with the larger waves is for values of $x_c = 1.04$ and $\eta(0) = 0.34$. The profile with the smaller waves is for values of $x_c = 4.45$ and $\eta(0) = 0.28$. (*b*) Weakly nonlinear phase portrait for (*a*). (*c*) Weakly nonlinear profiles; $\eta(x_c) = 0.09$. The profile with the larger waves is for values of $x_c = 1.21$ and $\eta(0) = 0.17$. The profile with the smaller waves is for values of $x_c = 4.72$ and $\eta(0) = 0.25$. (*d*) Weakly nonlinear phase portrait for (*c*).

Figure 2(*e*) is a computed fully nonlinear profile for values of F, α and β similar to those used in the weakly nonlinear profile of figure 2(*c*). The number of independent parameters is three, as suggested by the weakly nonlinear phase plane analysis, but it is more convenient to choose them as F, α, and ϕ_c (which essentially is the same as choosing x_c) in the nonlinear computations. Figure 2(*f*) is a plot of the nonlinear phase trajectories $\mathrm{d}y/\mathrm{d}x$ versus $y - 1$ for figure 2(*e*) and provides a check that the weakly nonlinear analysis in the phase plane is correct in figure 2(*d*). The agreement between the nonlinear and weakly nonlinear profiles in figure 2(*c*,*e*) is excellent for similar values of the parameters F, α and β, and it is even better for values of F closer to 1.

3.2. *Generalized critical flow*

We now consider generalized critical flows. Then the flow is uniform as $x \to \infty$ with $F > 1$ and characterized by a train of waves as $x \to -\infty$. The weakly nonlinear analysis shows that the solutions depend on four parameters. These parameters are chosen as $F > 1$, α, β and x_c.

Typical weakly nonlinear profiles together with their phase portraits are shown in figure 3. Here we start on a periodic orbit in the phase plane and then move to the homoclinic orbit along a straight line representing the curved plate G_1 (2.9). Finally we move along the homoclinic orbit to the saddle point.

As noted in the introduction the waves in figure 3 do not satisfy the radiation condition for flows from left to right. Dias & Vanden-Broeck (2004), Binder *et al.* (2005) and Binder & Vanden-Broeck (2007) showed that solutions satisfying the radiation

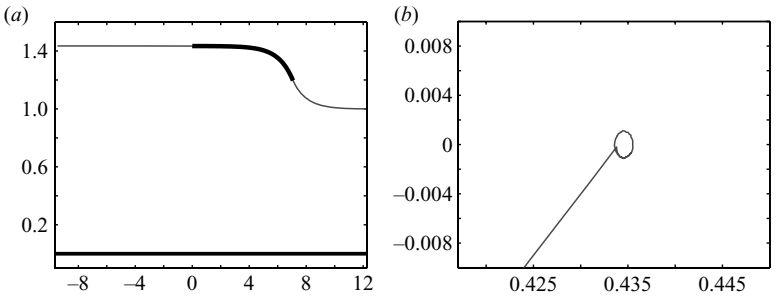

FIGURE 4. Generalized critical flow: $F = 1.3$, $\alpha = 1$, $\beta = -0.4340$, $x_c = 7.065$ ($\phi_c = 5$), $y(0) = 1.4338$, $y(x_c) = 1.1959$ and wave amplitude = 0.002. The shape of the curved plate is defined by G_1 (2.9). (*a*) Nonlinear profile. (*b*) Blow-up of the nonlinear phase trajectory for (*a*) near the centre.

condition can be obtained by introducing a second disturbance in the flow. An interesting question is whether or not solutions satisfying the radiation condition can be obtained without introducing a second disturbance but by choosing appropriately the shape of the curved plate. For the choice G_1 (2.9), figure 3 shows that the amplitude of the waves decreases as x_c increases. In fact these waves can be made arbitrarily small by taking the limit $x_c \to \infty$. This can be shown analytically as follows: For the waves to disappear, the straight line G_1 (2.9) has to pass through the centre. Therefore $\eta_x(0) = 0$, and (2.11) implies that x_c is unbounded. The problem with $x_c = \infty$ is that the free surface CD then disappears. We shall show in the next sections that waveless solutions with x_c finite can be constructed by choosing different shapes for the curved plate.

Shown in figure 4(*a*) is a computed nonlinear profile for the given values $F = 1.3$, $\alpha = 1$, $\beta = -0.4340$ and $\phi_c = 5$. It is qualitatively similar to the weakly nonlinear profiles shown in figure 3(*c*). The amplitude of the waves (0.002) is not visible in the profile of figure 4(*a*), but it is visible in figure 4(*b*) which is a blown-up plot of the nonlinear phase trajectories.

3.3. *Subcritical flow*

Subcritical flows are characterized by $F < 1$. The phase plane is sketched in figure 5(*b*). There is a centre at $(0, 0)$ and a saddle point at $(4(F-1)/3, 0)$. We need to combine the phase portrait with a line representing the plate. There are two cases.

The first case is a line joining the centre to a periodic orbit. This is the case illustrated in figure 5(*b*). The second case is a line joining two periodic orbits. There are then waves both far upstream and far downstream, and the radiation condition is therefore not satisfied.

In the first case we have a train of waves as $x \to -\infty$ and no waves as $x \to \infty$, provided x_c is finite (see figure 5*b*). A physical solution satisfying the radiation condition is then obtained by reversing the direction of the flow. For the choice G_1 (2.9), the condition $\eta_x(x_c) = 0$ and the relation (2.11) implies $x_c = \infty$ like in § 3.2. We now show that finite values of x_c can be obtained by using a different choice for $G(\eta)$, such as G_2 (2.9). We first note that (2.5) implies

$$x_c = \int_{\eta(0)}^{0} \frac{\mathrm{d}\eta}{G(\eta)}. \tag{3.1}$$

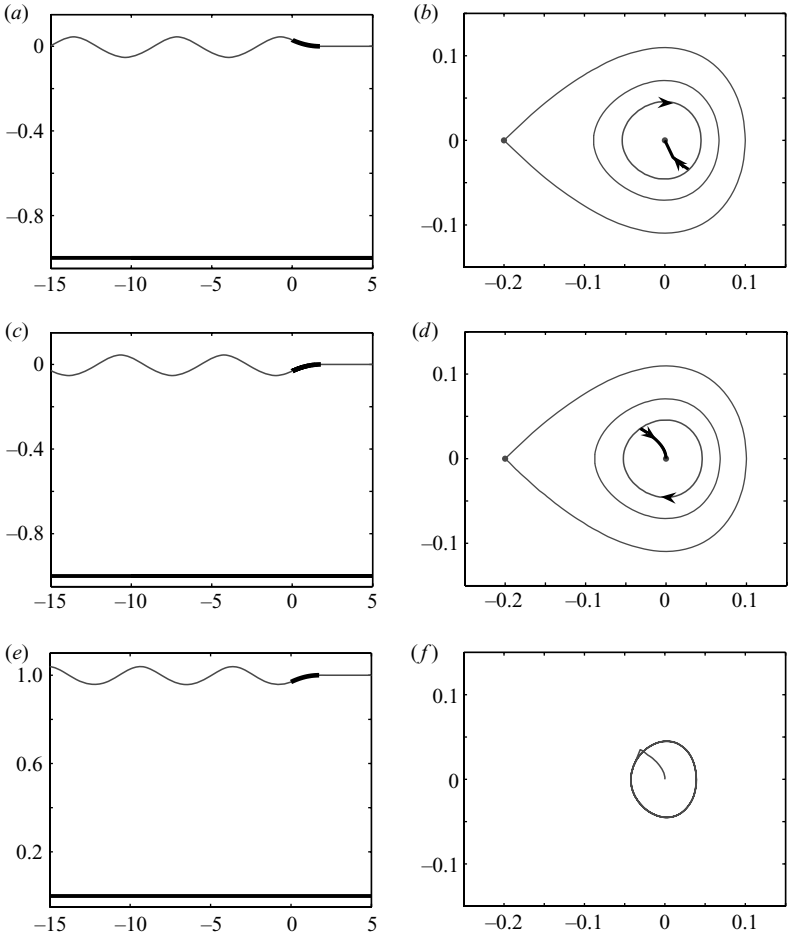

FIGURE 5. Subcritical flow, $F = 0.85$. The shape of the curved plate is defined by G_2 (2.9). (*a*) Weakly nonlinear profile, $\gamma = 0.01$, $x_c = 1.74$ and $\eta(0) = 0.03$. (*b*) Weakly nonlinear phase portrait for (*a*). (*c*) Weakly nonlinear profile: $\gamma = -0.01$, $x_c = 1.74$ and $\eta(0) = -0.03$. (*d*) Weakly nonlinear phase portrait for (*c*). (*e*) Nonlinear profile: $\gamma = -0.01$, $x_c = 1.75$ ($\phi_c = 1.75$) and $y(0) = 0.971$. (*f*) Nonlinear phase trajectory for (*e*).

The requirement that the line representing the plate go through the centre implies that $G(0) = 0$. We satisfy this condition by assuming that

$$G(\eta) \approx |\eta|^{\delta} \quad \text{as} \quad \eta \to 0, \tag{3.2}$$

where $\delta > 0$ is a given constant.

Using the relation (3.2) we find that x_c is unbounded when $\delta \geqslant 1$ because the integral in (3.1) is then divergent. Therefore the condition for x_c to be finite is $\delta < 1$.

To illustrate this we present in figure 5 results for a plate with shape G_2 (2.9). It follows that (3.2) is satisfied with $\delta = 0.5 < 1$ and

$$x_c = (\eta(0)/\gamma))^{1/2} \tag{3.3}$$

is finite. Note that the shape G_2 (2.9) has constant curvature $\eta_{xx} = 2\gamma$. As the curvature goes to 0, the plate becomes a flat horizontal plate.

Typical weakly nonlinear profiles together with their phase portraits are presented in figure 5(*a*)–(*d*). The number of independent parameters is three, and they can be taken as $F<1$, γ and x_c. We note that for fixed values of F and γ, increasing the value of x_c increases the amplitude of the waves.

Shown in figure 5(*e*, *f*) are a computed nonlinear profile and the corresponding phase trajectory for the same number of independent parameters as for the weakly nonlinear solutions of figure 5(*c*, *d*). There is excellent agreement between the weakly and fully nonlinear solutions.

Also, the sketch in figure 1 is a computed nonlinear profile for values of $F=0.50$, $\gamma=0.01$ and $x_c=1.75$. It is qualitatively similar to the weakly nonlinear solution of figure 5(*a*).

Since potential flows are reversible, the solutions of figures 1 and 5 are physical solutions satisfying the radiation condition when the direction of the flow is reversed. This is to be contrasted with the subcritical flows past a flat plate of Binder & Vanden-Broeck (2005) in which the radiation condition could not be satisfied.

3.4. *Waveless solutions and critical flows*

We now consider limit cases of the subcritical solutions of figure 5 for which the waves are eliminated on the free surface AB. Such flows are completely waveless and can be obtained by extending the line representing the plate in figure 5(*a*) up to the homoclinic orbit. Typical resulting weakly nonlinear solutions and their corresponding phase portraits are shown in figure 6(*a–d*). We start at the saddle point, move along the homoclinic orbit and then go to the centre along the line representing the plate. The solutions depend on two parameters which are chosen as F and γ. Figure 6(*e*) is a computed nonlinear solution for the same values of F and γ as in the weakly nonlinear profile (figure 6*c*), and figure 6(*f*) is a plot of the corresponding nonlinear phase trajectory. Consider now the control volume bounded by the bottom, the free surfaces, the plate and two cross-sections far upstream and far downstream. Applying the control volume to continuity and using Bernoulli's equation leads to the following exact relations:

$$F^{*}=F\left(\frac{V}{U}\right)^{3/2}=F\left(\frac{D}{H}\right)^{-3/2},\quad \frac{D}{H}=\frac{F^{2}}{4}\left(1+\sqrt{1+\frac{8}{F^{2}}}\right),$$
$$\frac{V}{U}=\frac{1}{2}\left(\sqrt{1+\frac{8}{F^{2}}}-1\right). \tag{3.4}$$

The radiation condition is satisfied in figure 6, since there are no waves on the free surfaces AB and CD. However for a physically realistic solution the flow direction needs to be reversed. Applying the control volume to horizontal momentum gives an exact expression for the horizontal force F_x exerted on the plate (per unit width):

$$F_x=\rho U^{2}H\left[\frac{5}{4}-\frac{1}{2}\sqrt{1+\frac{8}{F^{2}}}\left(1+\frac{F^{2}}{8}\right)-\frac{1}{2}\left(\frac{F^{2}}{8}-\frac{1}{F^{2}}\right)\right], \tag{3.5}$$

where ρ is the fluid density. The force increases from 0 to ∞ as the Froude number decreases from 1 to 0. For a flat plate Binder & Vanden-Broeck (2005) showed that there are no solutions for critical flows that satisfy the radiation condition. Here we have shown that such solutions exist for a curved plate. Finally let us mention that the flows in figure 6 (when reversed) can be viewed as particular cases of the generalized

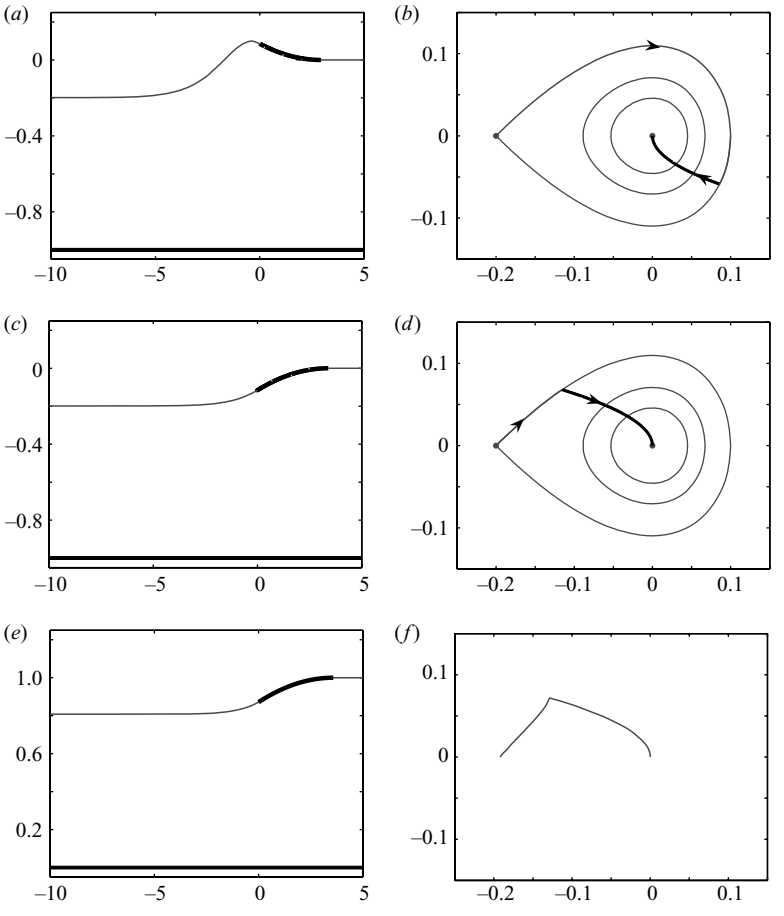

FIGURE 6. Waveless flow: $F = 0.85$. The shape of the curved plate is defined by G_2 (2.9). (*a*) Weakly nonlinear profile: $\gamma = 0.01$, $x_c = 3.00$ and $\eta(0) = 0.09$. (*b*) Weakly nonlinear phase portrait for (*a*). (*c*) Weakly nonlinear profile: $\gamma = -0.01$, $x_c = 3.46$ and $\eta(0) = -0.12$. (*d*) Weakly nonlinear phase portrait for (*c*). (*e*) Nonlinear profile: $\gamma = -0.01$, $\phi_c = 3.73$ ($x_c = 3.58$) and $y(0) = 0.871$. The exact formula (3.4) gives 0.8082 for the free-surface elevation on the left, in excellent agreement with the numerical result. (*f*) Nonlinear phase portrait for (*e*).

critical flows for which the waves have been eliminated by an appropriate choice of the shape of the curved plate.

The overall conclusion is that the existence of subcritical and critical flows for certain types of curved plates is not due to the curvature (both shapes G_1 and G_2 have non-zero curvature but only G_2 can provide these flows) but rather due to the behaviour $G(\eta) \approx |\eta|^{\delta}$ as $\eta \to 0$ (3.2), with $0 < \delta < 1$. This behaviour implies that the plate connects horizontally with the free surface at one end. Future work will be devoted to a deeper underlying physical explanation.

REFERENCES

ASAVANANT, J. & VANDEN-BROECK, J.-M. 1994 Free-surface flows past a surface-piercing object of finite length. *J. Fluid Mech.* **273**, 109–124.

BINDER, B. J., DIAS, F. & VANDEN-BROECK, J.-M. 2005 Forced solitary waves and fronts past submerged obstacles. *Chaos* **15**, 037106.

Binder, B. J., Dias, F. & Vanden-Broeck, J.-M. 2006 Steady free-surface flow past an uneven channel bottom. *Theor. Comp. Fluid Dyn.* **20**, 125–144.

Binder, B. J. & Vanden-Broeck, J.-M. 2005 Free surface flows past surfboards and sluice gates. *Eur. J. Appl. Math.* **16**, 601–619.

Binder, B. J. & Vanden-Broeck, J.-M. 2007 The effect of disturbances on the flow under a sluice gate and past an inclined plate. *J. Fluid Mech.* **576**, 475–490.

Budden, P. J. & Norbury, J. 1977 Sluice-gate problems with gravity. *Math. Proc. Camb. Phil. Soc.* **81**, 157–177.

Dias, F. & Vanden-Broeck, J.-M. 2002 Generalized critical free-surface flows. *J. Engng Math.* **42**, 291–301.

Dias, F. & Vanden-Broeck, J.-M. 2004 Trapped waves between submerged obstacles. *J. Fluid Mech.* **509**, 93–102.

Fridman, G. M. & Tuck, E. O. 2006 Two-dimensional finite-depth planing hydrofoil under gravity. *Proc. Third International Summer Scientific School, "High Speed Hydrodynamics and Numerical Simulation", Kemerovo, Russia.*

Forbes, L.-K. 1988 Critical free-surface flow over a semi-circular obstruction. *J. Engng Math.* **22**, 3–13.

King, A. C. & Bloor, M. I. G. 1987 Free-surface flow over a step. *J. Fluid Mech.* **182**, 193–208.

Shen, S. S-P. 1995 On the accuracy of the stationary forced Korteweg–de Vries equation as a model equation for flows over a bump. *Q. Appl. Math.* **53**, 701–719.

Vanden-Broeck, J.-M. 1997 Numerical calculations of the free-surface flow under a sluice gate. *J. Fluid Mech.* **330**, 339–347.

Vanden-Broeck, J.-M. & Keller, J. B. 1989 Surfing on solitary waves. *J. Fluid Mech.* **198**, 115–125.